Supporting Information

Few-layered MoS_2 Nanosheets Wrapped Ultrafine TiO_2 Nanobelts with Enhanced Photocatalytic Property

Haidong Li[1¶], Yana Wang[1¶], Guohui Chen[1], Yuanhua Sang[1], Huaidong Jiang[1], Jiating He[2], Xu Li[2*] and Hong Liu[1*]

1. State Key Laboratory of Crystal Materials, Shandong University, Jinan 250100 China

2. Institute of Materials Research and Engineering, A*STAR, 2 Fusionopolis Way, Innovis, #08-3, Singapore 138634.

¶ These authors have contributed equally to this work.

* Corresponding authors: hongliu@sdu.edu.cn (H. Liu), x-li@imre.a-star.edu.sg (X. Li)

S1 Morphology of ultrafine TiO_2 nanobelts and MoS_2/TiO_2 nanobelt heterostructures

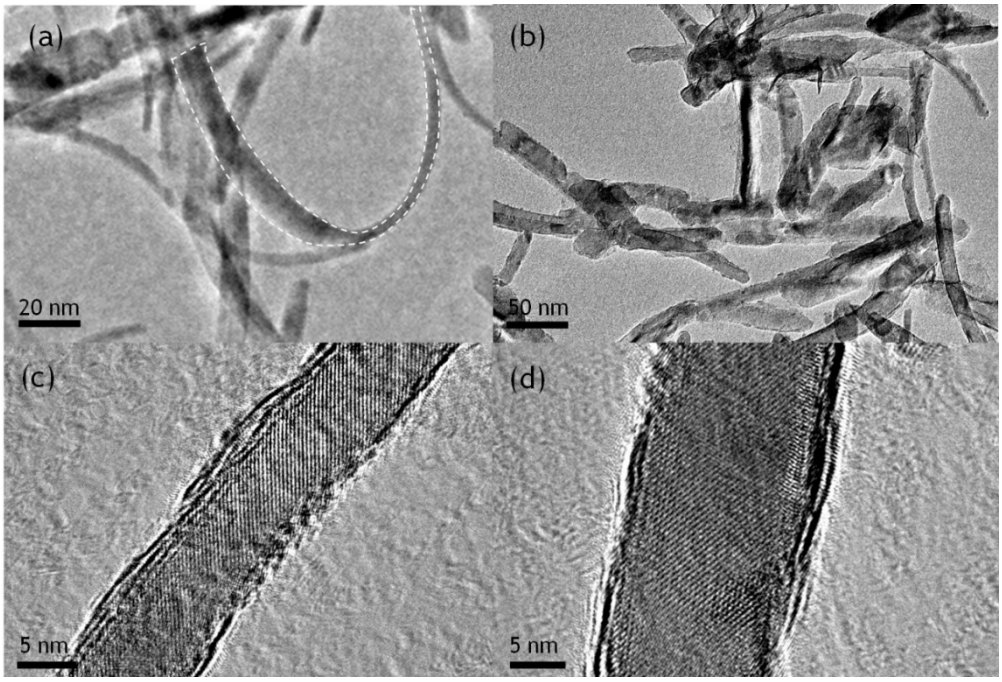

Figure S1 Morphology of ultrafine TiO_2 nanobelts and MoS_2/TiO_2 nanobelt heterostructures: (a) TEM image of ultrafine TiO_2 nanobelts, (b) (c) and (d) TEM and HRTEM images of MoS_2/TiO_2 nanobelt heterostructures (5% of MoS_2).

Figure. S1 (a) shows the morphology of ultrathin TiO_2 nanostructures with DMF/HAc to be 6/4 (v/v). It is observed that the ultrafine TiO_2 nanostructures are very flexible and the they are confirmed to be ultrathin with no more than 5 nm in thickness and 10-20 nm in width and hundreds nm in length.

TEM and HRTEM images of MoS_2/TiO_2 nanobelt heterostructures are shown in Figure S1 (b), (c) and (d). The thickness of the MoS_2 sheets is measured as about 1.4 nm or 2.2 nm, indicating that the some nanosheets are multilayer MoS_2 nanosheets[1-4].

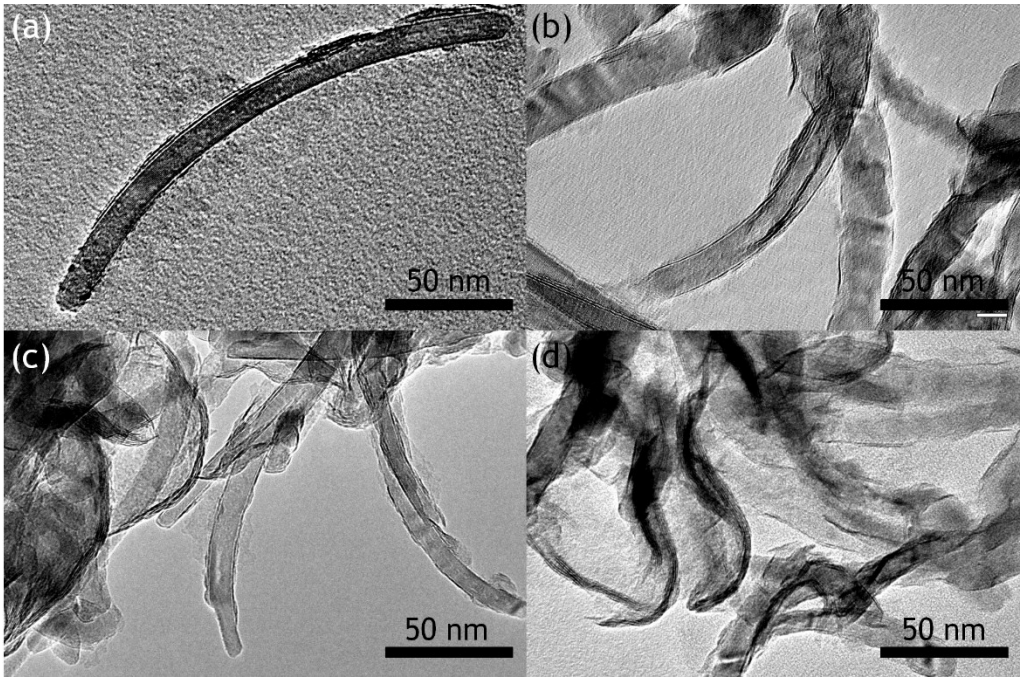

Figure S2. TEM images of MoS_2/TiO_2 hybrid nanobelt with different MoS_2 loading amount: (a) 2%, (b) 5 % (c) 10% and (d) 50%

Figure S2 shows the TEM images of MoS_2/TiO_2 hybrid nanobelt with different MoS_2 loading amount: (a) 2%, (b) 5 % (c) 10% and (d) 50%. As shown in Figure S2a, layered MoS_2 nanosheets partly wrapped on the surface of ultrafine TiO_2 nanobelts is present. With MoS_2 loading amount increase to 5%, layered crystal structure fully wrapped on the surface of ultrafine TiO_2 nanobelts is present (Figure S2b). So the fully wrapped MoS_2/TiO_2 hybrid nanobelts are selected, which possess the highest photocatalytic performance (see Figure S4). When MoS_2 loading amount increases to 10% and 50%,

overmuch MoS_2 naonosheet or multilayered MoS_2 grown on the naonobelts (Figure S2c and S2d). Which weaken their photocatalytic performance.

S2 EDS results from MoS_2/TiO_2 nanobelt heterostructures

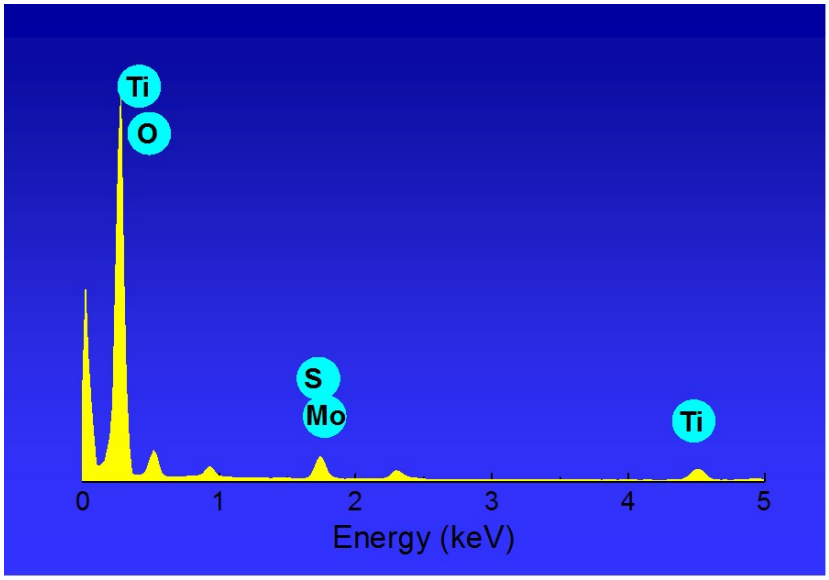

Figure S3 EDS results from MoS_2/TiO_2 nanobelt heterostructures (5% of MoS_2).

Energy dispersive X-ray spectrometry (EDS) results of an MoS_2/TiO_2 nanobelt heterostructures with individual elements of Mo, S, Ti and O (Figure S3) further confirm that the hybrid hierarchical structure where the outer layer is MoS_2 nanosheets and the inter layer is TiO_2 nanobelt.

S3 Degradation of MO for MoS_2/TiO_2 nanobelt heterostructures

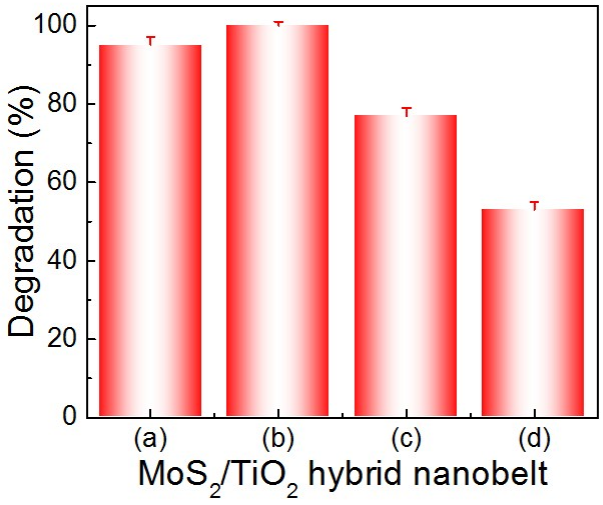

Figure S4. Comparisons of photocatalytic activities among the MoS_2/TiO_2 samples with different weight ratios with different MoS_2 loading amount: (a) 2%, (b) 5 % (c) 10% and (d) 50% under UV light irradiation in 15 min.

As shown in Figure 6a in the main text, in the presence of pure TiO_2 nanobelt, about 92.4% of MO is degraded within 15 min, while the degradation ratio is of 100% in the presence of the MoS_2/TiO_2 hybrid nanobelts. For MoS_2/TiO_2 hybrid nanobelts with increasing MoS_2 loading amount of MoS_2, the photocatalytic performance decreases and the optimized MoS_2 loading amount is 5% (Figure S4).This is attributrd to layered MoS_2 nanosheets fully wrapped on the surface of ultrafine TiO_2 nanobelts.

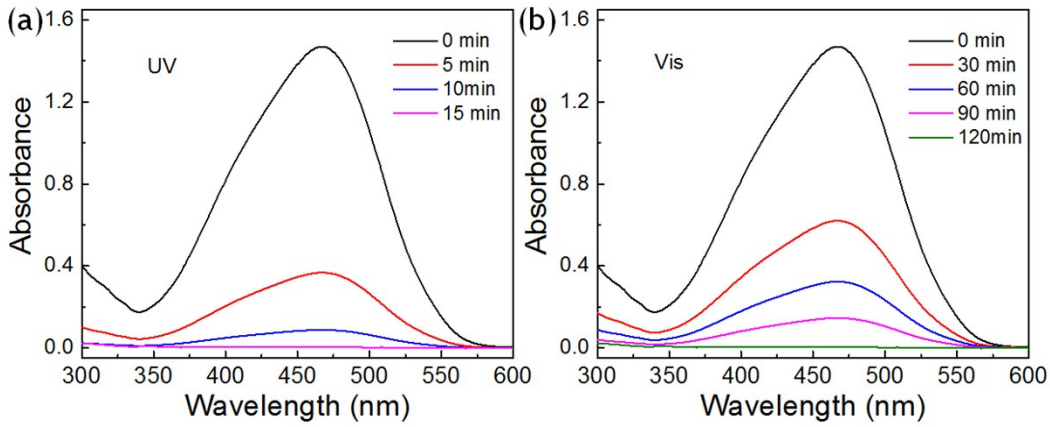

Figure S5 Absorption spectra of MO solution during the photocatalytic degradation under (a) UV and (b) visible light irradiation treatment in presence of MoS_2/TiO_2 nanobelt heterostructures

Figure S5 shows the absorption spectra of methylene orange (MO) solution during the photocatalytic degradation under (a) UV and (b) visible light irradiation treatment in presence of MoS_2/TiO_2 nanobelt heterostructures. From Figure S5, it can be observed that the photocatalytic degradation rate can reach 100% under either (a) UV or (b) visible light irradiation.

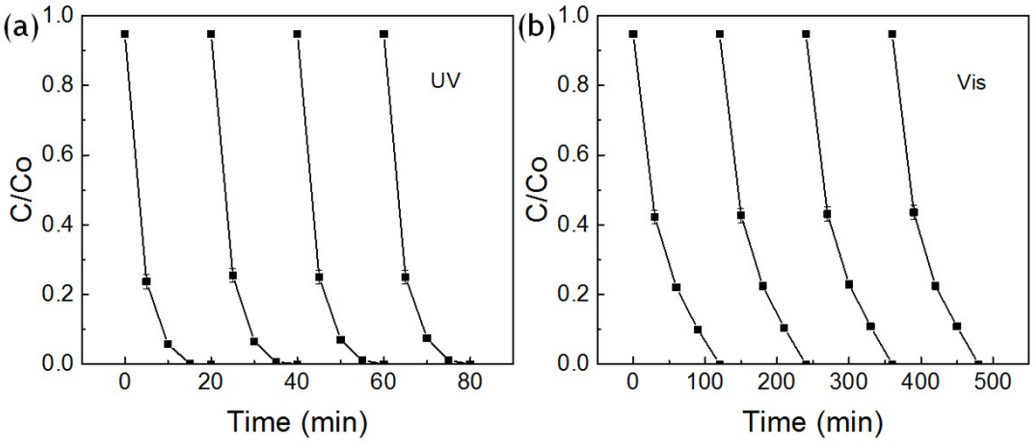

Figure S6 Photocatalytic degradation of MO by the MoS_2/TiO_2 nanobelt heterostructures in repeated experiments under (a) UV and (b) visible light irradiation.

To examine the photocatalytic stability of the catalysts, the efficiency of the MO photodegradation was evaluated in a repetitive mode using the same photocatalysts. As shown in Figure S6 a and b, the MO dye was quickly decomposed after every injection of the MO solution and the MoS_2/TiO_2 nanobelt heterostructures are stable under repeated experiments with a nearly constant photodecomposition rate. Thus, the MoS_2/TiO_2 nanobelt heterostructures are an effective and stable photocatalyst under UV and visible light irradiation.

S4 Photocatalytic H_2 evolution from an aqueous methanol solution

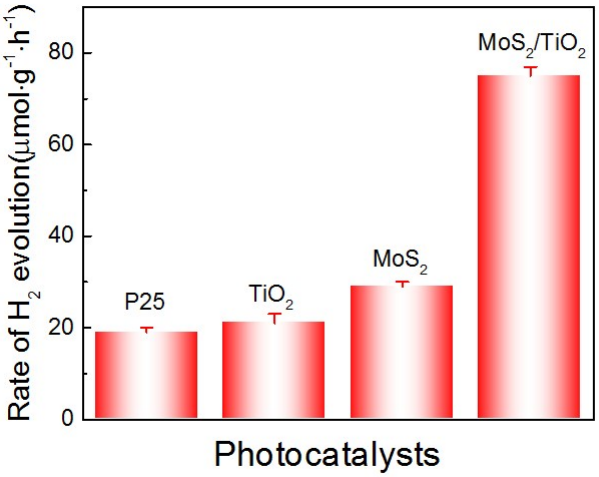

Figure S7 Comparison of the photocatalytic hydrogen evolution activities of different samples.

For comparison, the photocatalytic activities of pure P25, ultrafine TiO_2 nanobelts and MoS_2 are also displayed. To check the intrinsic photocatalytic property of the samples,

noble nanoparticles were not sputtered on the samples before hydrogen generation measurement. Figure S7 illustrates the hydrogen evolution from an aqueous solution containing methanol as sacrificial agents. Under irradiation of simulated light, The hydrogen generation rate of the MoS_2/TiO_2 nanobelt heterostructures is about 75 μmol•h^{-1}•g^{-1}, while the hydrogen generation rate of the P25, TiO_2 nanobelts and MoS_2 nanosheets is about 29 μmol•h^{-1}•g^{-1},21 μmol•h^{-1}•$g^{-1}$and 19 μmol•h^{-1}•g^{-1}, respectively.

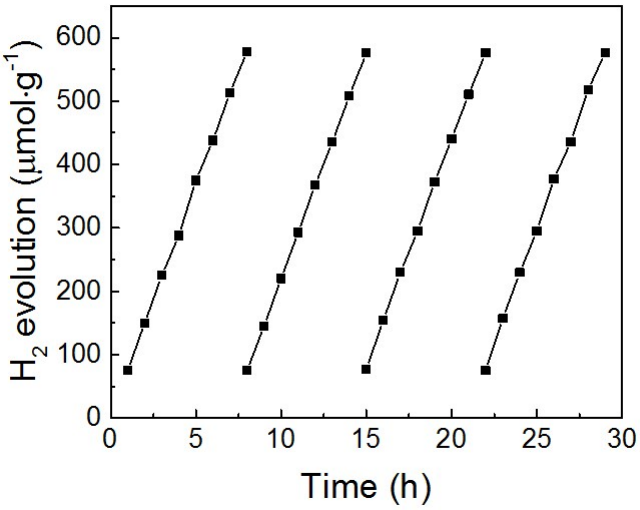

Figure S8 Photocatalytic H_2 evolution in 8 h repeated cycles by the MoS_2/TiO_2 nanobelt heterostructures.

Repetitive photocatalytic H_2 evolution from an aqueous methanol solution for the MoS_2/TiO_2 nanobelt heterostructures is shown in the Figure S8. After four cycles of 8 h reaction, the MoS_2/TiO_2 nanobelt heterostructures still retained high photocatalytic activity, which demonstrates their stability.

S5 Schematic illustration of photo-induced charge transfer and separation

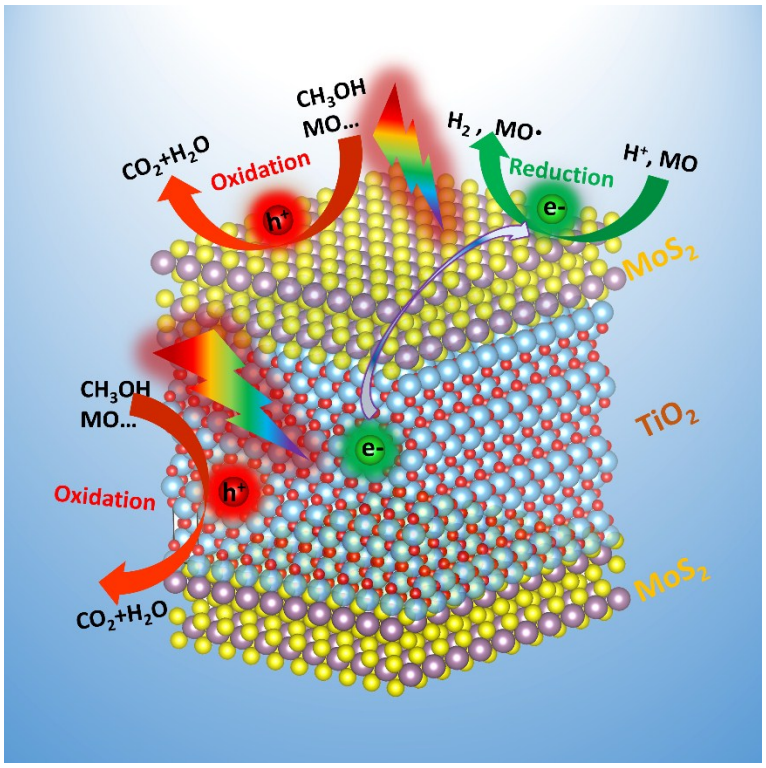

Figure S9 Schematic illustration of the charge transfer in MoS_2/TiO_2 hybrid nanobelt.

A tentative mechanism proposed for the H_2 production and pollutant degradation based on the occurrence of vectorial electrons and holes transfer in MoS_2/TiO_2 hybrid nanobelt was shown in Figure S9. Under light irradiation, the photogenerated electrons from the valence band (VB) of MoS_2 nanoparticles are directly transferred to conduction band (CB) of MoS_2, and leaving behind holes in the VB[5-7]. As the CB of TiO_2 is lower than that of MoS_2, the TiO_2 can be used as a photoelectronic acceptor, the photogenerated electrons of the MoS_2 CB will be transferred to the CB of TiO_2 nanobelts. The photogenerated electrons can be trapped by oxygen molecules in the aqueous solution to form singlet oxygen. Simultaneously, the holes moved in the opposite direction from the electrons, photogenerated holes will be captured within the MoS_2 nanosheets. The photogenerated

electrons and holes can be separated effectively and improve the photocatalytic activity of MoS_2/TiO_2 nanobelt heterostructures.

Reference

1. M. Shen, Z. Yan, L. Yang, P. Du, J. Zhang and B. Xiang, *Chemical communications*, 2014, **50**, 15447-15449.
2. Y. Song, Y. Lei, H. Xu, C. Wang, J. Yan, H. Zhao, Y. Xu, J. Xia, S. Yin and H. Li, *Dalton transactions*, 2015, **44**, 3057-3066.
3. J. Liu, Z. Zeng, X. Cao, G. Lu, L. H. Wang, Q. L. Fan, W. Huang and H. Zhang, *Small*, 2012, **8**, 3517-3522.
4. Z. Yin, Z. Zeng, J. Liu, Q. He, P. Chen and H. Zhang, *Small*, 2013, **9**, 727-731.
5. X. Sun, J. Dai, Y. Guo, C. Wu, F. Hu, J. Zhao, X. Zeng and Y. Xie, *Nanoscale*, 2014, **6**, 8359-8367.
6. Y. Zhu, Q. Ling, Y. Liu, H. Wang and Y. Zhu, *Physical chemistry chemical physics : PCCP*, 2015, **17**, 933-940.
7. Y. Li, Y.-L. Li, C. M. Araujo, W. Luo and R. Ahuja, *Catalysis Science & Technology*, 2013, **3**, 2214.